Solar System Data Mules: Analysis for Mars and Jupiter

Marc Sanchez Net
Jet Propulsion Laboratory
California Institute of Technology,
Pasadena, California, 91109
marc.sanchez.net@jpl.nasa.gov

Etienne Pellegrini
Jet Propulsion Laboratory
California Institute of Technology,
Pasadena, California, 91109
pellegrini@jpl.nasa.gov

Wilson Parker
Jet Propulsion Laboratory
California Institute of Technology,
Pasadena, California, 91109
wilson.p.parker@jpl.nasa.gov

Joshua Vander Hook
Jet Propulsion Laboratory
California Institute of Technology,
Pasadena, California, 91109
hook@jpl.nasa.gov

Abstract—**This paper explores the ability to ferry data between Mars and Earth, and Jupiter and Earth, using a network of small spacecraft (termed "data mules") placed in phase-shifted cycler orbits between both planets. These cycler orbits enable the data mules to periodically visit the destination planet without requiring large amounts of fuel. However, their long periodicity also limits the cadence of visits since several years may elapse between consecutive data mule flybys.**

To increase total data return to Earth, we compare two alternative concepts of operations. First, we assume that each data mule carries an optical terminal capable of establishing a very high-rate inter-satellite link with a spacecraft orbiting Mars and Jupiter (where all data to be returned is stored). This inter-satellite link operates for a short period of time, nominally during 1 day around closest approach of the data mule to the planetary body of interest. This is compared to normal Deep Space Network (DSN) operations, in which we optimistically assume a continuous direct-to-Earth link with a ground antenna. Through our analysis, we show that the concept of data mules can substantially increase the total amount of data returnable from planetary bodies when used as a complement to current DSN support. We also show how the system performance, measured in terms of total returnable data volume or amortized yearly data rate, depends on technological constraints to implement the deep space and proximity links, as well as geometrical constraints imposed by cycler orbits and the solar system.

TABLE OF CONTENTS

1. INTRODUCTION

Returning large data volumes from bodies far into the solar system is challenging due to the enormous propagation distances that the signal needs to travel. For instance, in the case of RF communications with an infinite-bandwidth additive white Gaussian noise (AWGN) channel, it is well-known that the supportable data rate decreases as $1/d^2$ [1]. Similar results are also true for photon-efficient optical communications using Pulse Position Modulation (PPM), for which the link rate scales initially as $1/d^2$, and even transitions to scaling as $1/d^4$ after a critical distance of 1 AU approximately [1].

Given the strong dependence of link rate with distance, a sensible approach to achieve petabit scale data transfers between two distant objects is to avoid propagating electromagnetic waves in free space over very long distances. Therefore, this paper studies the feasibility and limits of petabit scales transfers between Earth and a planetary body using the concept of data mules, i.e. a network of smallsats placed in cycler orbits that visit both planets periodically to first collect and then dump data over short-range links [2]. This concept is newly enabled by high speed optical communications and the availability of CubeSat and smallsat secondary payloads, and builds upon previous space logistics problems that leverage cycler orbits between Mars and Earth.

In our previous paper, we showed that it is possible to build a network of data mules that visit Mars with quasi-regular cadence to collect vasts amounts of data using an optical intersatellite between the mule and a Mars orbiter [2]. To do so, we made reasonable assumptions of the technology available for the intersatellite link using current flight optical terminals such as JPL's Deep Space Optical Communications terminal and NASA's Lunar Laser Communication Demonstration (LLCD) terminal. Since optical technology for space communications is an area of active research and development, in this paper we ask the question of what is the maximum achievable data transfer possible using data mules. To answer it, we first estimate the total data volume returnable from Mars and Jupiter over a synodic period assuming a noise-free optical crosslink with minimal constraints on modulation and coding. We then compare this value with the total data volume that would have been returned to Earth if the orbiter had been continuously supported by the DSN.

2. PRELIMINARIES

Capacity of RF links

We first consider the maximum achievable data rate for a direct-to-Earth (DTE) link between the DSN and an planetary orbiter. Shannon derived that the maximum achievable rate in an AWGN channel with finite bandwidth W can be estimated

978-1-7281-7436-5/21/$31.00 ©2021 IEEE

as

$$C_{\text{rf}}^{\text{W}} = W \log_2 \left(1 + \frac{P_r}{N_0 W}\right), \tag{1}$$

in bits per second, where P_r denotes the received power and N_0 is the noise spectral density. In the case of infinite bandwidth, i.e., $W \to \infty$, this equation reduces to

$$C_{\text{rf}}^{\text{U}} = \frac{P_r}{\ln(2) N_0}, \tag{2}$$

also in bits per second, which represents the channel capacity without bandwidth constraints.

To quantify the dependence between link capacity and link distance, we utilize the well-known link budget equation in its linear form [3]. In particular, the received average signal power can expressed as

$$P_r = \frac{P_t G_t G_r}{L L_{\text{fs}} M}, \tag{3}$$

where P_t is the transmitted power, G_t is the transmitter antenna gain, G_r is the receiver gain, L_{fs} represents the free space losses, and L is a lumped loss term that accounts for all implementation, atmospheric, pointing and polarization losses. Finally, it is customary in link budgets to set a constant link margin M, which we set to 3 dB.

Assuming that the receiver is on the ground and uses a directional antenna, and knowing that the maximum antenna gain is related to its effective aperture A_e by the constant $\frac{4\pi}{\lambda^2}$, we can rewrite the link budget equation as follows:

$$\frac{P_r}{N_0} = \gamma_{RF} \, \text{EIRP} \frac{A_e}{T} \frac{1}{d^2}, \tag{4}$$

where $\gamma_{RF} = \frac{1}{4\pi k L M}$ is a constant. In equation (4) we have used the fact that for thermal noise the spectral power density can be approximated as kT, where k is the Boltzmann constant and T is the equivalent receiver temperature, which we assume constant. Also, (4) divides the terms of the link budget equation in four categories:

- γ_{RF} is a lump *constant* that depends on losses, physical constants, and the link margin;
- EIRP is the transmitter's characteristic figure of merit. It indicates how well electromagnetic power is radiated onto free space;
- A_e/T is the receiver's characteristic figure of merit. It indicates how well the receiver collects electromagnetic power;
- finally, the term $1/d^2$ scales the received power by the link distance.

Finally, substituting equation (4) into equation (2), we get

$$C_{\text{rf}}^{\text{U}} = \frac{\gamma_{RF}}{\ln 2} \text{EIRP} \frac{A_e}{T} \frac{1}{d^2}, \tag{5}$$

which proves that the achievable link data rate is inversely proportional to the square of the link distance. The same procedure can be used to combine equations (1) and (4) to obtain C_{rf}^{W} as a function of distance, a result not reported here for brevity.

Ultimate Capacity of Optical Links

Having summarized the capacity of RF links, we now focus our attention on optical links. To facilitate the analysis, but also because we are interested in determining upper bounds for the performance of the proposed data mules concept, we start by considering the ultimate capacity of an optical link, which is derived assuming a noiseless channel and no signal format constraints other than the mean number of received signal photons per symbol n_s. This capacity is given by [4]

$$\tilde{C}_{\text{opt}}^{\text{ult}} = (1 + n_s) \log_2 (1 + n_s) - n_s \log_2 n_s \tag{6}$$

bits per channel use. Adding a bandwidth constraint such that the channel can only be used every T_s seconds, we get the ultimate optical capacity in bits per second

$$C_{\text{opt}}^{\text{ult}} = \frac{\tilde{C}_{\text{opt}}^{\text{ult}}}{T_s}. \tag{7}$$

Next, we estimate the average number of photons incident on the receiver per symbol. To that end, we once again rely on the link budget equation which, in this case, can be expressed as [5]

$$P_r = \gamma_{opt} \cdot \text{EIRP} \cdot A_e \frac{1}{d^2}, \tag{8}$$

where γ_{opt} is a lump constant that includes polarization, pointing, atmospheric losses (if applicable), implementation efficiencies and link margin. The rest of terms are defined as in the RF case.[2] Furthermore, the average number of photons incident on the receiver per second λ_s can be simply estimated as the average received power, divided by the energy of a photon at the carrier wavelength [5]

$$\lambda_s = \frac{P_r}{E}, \tag{9}$$

where $E = \frac{\hbar c}{\lambda}$, $\hbar$ denotes the Plank constant and c is the speed of light in the vacuum. Therefore, the average number of photons in a symbol of duration T_s is simply

$$n_s = \tilde{\gamma}_{opt} \cdot \text{EIRP} \cdot A_e \frac{1}{d^2}, \tag{10}$$

with $\tilde{\gamma}_{opt} = \frac{\gamma_{opt}}{E} T_s$. Finally, substituting Equation (10) in Equation (7) yields an expression relating the capacity of an optical link with the distance between the transmitter and receiver, a step not provided here for simplicity.

Finally, in Appendix A we provide approximations for the ultimate optical capacity under small and large number of received signal photons. We show when $n_s \ll 1$ then $\tilde{C}_{\text{opt}}^{\text{ult}} \approx n_s / \ln 2$ bits per channel use, which results in

$$C_{\text{opt}}^{\text{ult}} \approx \frac{\gamma_{opt}}{\ln(2) E} \cdot \text{EIRP} \cdot A_e \frac{1}{d^2}. \tag{11}$$

Just as before, this indicates that the supportable link rate will scale inversely proportional to the distance squared. Alternatively, when $n_s \gg 1$ then

$$\begin{aligned} C_{\text{opt}}^{\text{ult}} &\approx \frac{1}{\ln 2} + \log_2 n_s \\ &= \frac{1}{\ln 2} + \log_2 (\tilde{\gamma}_{opt} \cdot \text{EIRP} \cdot A_e) - 2 \log_2 d \end{aligned} \tag{12}$$

[2]Note that unlike γ_{RF}, γ_{opt} does not depend on the Boltzmann constant since we assumed the link to be noise-free.

and, therefore, the data rates scales logarithmically with distance.

Returnable Data Volume using the DSN

In the data mules concept, we assume that the spacecraft around the planetary body gathers large amounts of data, either because of its instruments, or because it serves as a data storage unit for other smaller less capable spacecraft. Furthermore, we assume that if normal operations were to be conducted with the DSN, the spacecraft would have a continuous link with Earth operating at its maximum achievable data rate. In other words, the total data volume returnable over a time horizon T, would simply be calculated as

$$DV_{\text{dsn}} = \int_{t_0}^{t_0+T} C_{\text{rf}}(t)dt, \tag{13}$$

where t_0 is an arbitrary point in time, and $C_{\text{rf}}(t)$ is the capacity of the deep space channel between Earth and the planetary body. Furthermore, using the assumptions from Section 2, $C_{\text{rf}}(t)$ depends on time solely because of changes in distance between the two planets. Also, its functional form is dictated by whether we consider the bandwidth constraint to be active or not — see Equation (1) vs. (2).

Returnable Data Volume using Data Mules

We now consider how operations would be conducted if a network of data mules were already in place and operating at full capacity. In that case, we assume that the orbiter around the planetary body of interest would operate as follows: During a normal day, it would maintain a continuous link with the DSN to return to Earth as much data as possible. Alternatively, during a close flyby by a data mule, the orbiter would cease transmission to Earth (except for low rate telemetry, if necessary) and, instead, reorient itself to establish a high data rate optical link. This intersallite link would be active for Δt seconds, after which the orbiter would resume normal DSN operations and the data mule would start its journey back to Earth.

Given this concept of operations, the total data volume returnable to Earth using our data mules concept can be estimated as

$$DV_{\text{dm}} = \int_{t_0}^{t_1} C_{\text{rf}}(t)dt + \int_{t_1}^{t_2} C_{\text{opt}}(t)dt + \int_{t_2}^{T} C_{\text{rf}}(t)dt, \tag{14}$$

where $t_2 = t_1 + \Delta t$, $C_{\text{rf}}(t)$ is defined as before, and $C_{\text{opt}}(t)$ is the capacity of the optical link as given by Equation (7). Equation (14) can also be easily modified to accommodate multiple flybys over the orbiter's lifetime, a step we obviate here for simplicity.

Data Mules Value Proposition

The proposed data mules concept will enhance the orbiter's operations and science return if the amount of data volume returnable over the its lifetime exceeds the amount of data that it could have been returned to Earth had it been operated via a deep space link with the DSN. Therefore, our proposed figure of merit for the system is simply the ratio of total returnable data volume:

$$\beta\left(t_1, t_2\right) = \frac{DV_{\text{dm}}}{DV_{\text{dsn}}} = \frac{\xi + \int_{t_1}^{t_2} C_{\text{opt}}(t)dt}{\xi + \int_{t_1}^{t_2} C_{\text{rf}}(t)dt}, \tag{15}$$

where

$$\xi(t_1, t_2) = \int_{t_0}^{t_1} C_{\text{rf}}(t)dt + \int_{t_2}^{T} C_{\text{rf}}(t)dt \tag{16}$$

is a constant that indicates the amount of data returned when the orbiter is not in contact with the data mule. Furthermore, and assuming that the data mule flyby is short in duration (e.g., one day or less), the distance between Earth and the planetary body of interest is approximately constant. Therefore,

$$\int_{t_1}^{t_2} C_{\text{rf}}(t)dt \approx \int_{t_1}^{t_2} C_{\text{rf}}(t_1)dt = C_{\text{rf}}(t_1)\Delta t, \tag{17}$$

where we have approximated the DTE link rate as constant and equal to what is achievable at the start of the contact. Consequently,

$$\beta\left(t_1, t_2\right) \approx \frac{\xi + \int_{t_1}^{t_2} C_{\text{opt}}(t)dt}{\xi + C_{\text{rf}}(t_1)\Delta t}. \tag{18}$$

Equation (18) can now be used to qualitatively understand how the value proposition of our data mule concept depends on the relative phase between the cycler orbit, and the synodic cycle between Earth and the planetary body of interest. Indeed, if the cycler arrives to the planet at maximum Earth-Planet distance, then $C_{\text{rf}}(t_1)$ is minimal and, consequently, β is maximal.

Similarly, Equation (18) can also be used to estimate the optimal duration of the intersatellite link between the orbiter and the data mule. In particular, we show in Appendix B that the conditions to determine the optimal t_1 and t_2 simply reduce to

$$C_{\text{rf}}(t_i) = C_{\text{opt}}(t_i), \tag{19}$$

with $i = 1$ or $i = 2$ depending on whether we are interested in the start or end of the intersatellite link. Note that this result is highly intuitive: The moment in time t_1 where we should transition from the DTE link, to the orbiter-data mule link occurs when the supportable data rate in the latter links starts to exceed the data rate supportable in the deep space link (and vice versa for t_2). Note also that in real operations t_1 and t_2 might be set by factors that are independent from returnable data volume (e.g., cycler orbit characteristics, limitations on the optical terminals, orbiter operational constraints, etc.). Yet, this simple analysis yields enough insight that we can now use its tenets to guide the search for "good" cycler orbits and design the crosslinks between orbiter and the data mule.

3. LINK BUDGET ASSUMPTIONS

This section specifies the link budget assumptions we make for our analysis of the data mules concept. In particular, we focus our attention on two links: the RF DTE link between the Orbiter and the DSN; and the optical crosslink between the orbiter and the data mule. Note that a third link between the data mule and Earth is necessary for successful return of data to Earth. However, we consider this a supporting link that is sized to match the crosslink between the data mule and the orbiter. Therefore it is left outside of the scope of this paper.

Direct-to-Earth Link

For the purposes of this article, we assume that the DTE link betweem the orbiter and the DSN operates at Ka-band (32 GHz). This results in:

The total system losses (excluding free space propagation) are estimated at -7.65 dB, including -1.2 dB of atmospheric loss based 95% confidence weather in a DSN site [6]. Additionally, we assume a 3 dB link margin and a 1 dB coding gap.

The effective area divided by system noise temperature A_e/T of a DSN station depends on whether a 34 or 70 meter is used to establish the DTE link. For the DSN 34m antennas, we estimate its value at 12 dB-m^2/K. Therefore, since the 70m has four times more collective area, its A_e/T is estimated at 18 dB-m^2/K (similar performance would also be obtained by arraying four 34m antennas).

The EIRP of the orbiter depends on the spacecraft transmitted power and antenna gain. Assuming a 3m antenna and 20 W of transmit power, we expect an EIRP of 70.45 dBW.

These numbers can be directly substituted into Equation (5) to obtain

$$R_{\text{rf}}^{\text{u}} \qquad \frac{4.79 \quad 10^7}{d^2} \text{ bps}, \tag{20}$$

where d is expressed in astronomical units. Note that this value is now an effective link data rate since a coding gap of 1 dB has been assumed.

Figure 1 plots the data rate supportable between Earth and Mars, and Earth and Jupiter, for the current decade (2020 to 2030). Observe that for Mars, the maximum data rate is almost two orders of magnitude larger than the minimum data rate (275 vs. 7 Mbps). Additionally, the peak data rate only occurs for very short periods of time. This indicates that, in order to maximize β, the data mule orbit needs to ideally be designed so that Mars flybys do not occur close to solar opposition. In contrast, the data rate variation for Jupiter only ranges from 1.15 to 3.1 Mbps. Therefore, the exact phase of the cycler orbit with respect to the Earth-Jupiter synodic cycle is likely to have a minor impact on β.

Optical Crosslink

Next, we consider the performance of the optical crosslink. To that end, we make the following assumptions:

The total system losses (excluding free space propagation) are estimated at -8.17 dB. This includes a 3 dB margin, a 2 dB coding gap, a 3 dB fiber coupling loss, and a relative depointing of 7% at both the transmit and receive telescopes.

The effective area of the receive aperture is assumed to be 0.027 m^2 based on a 0.1 m telescope with 35% efficiency.

The EIRP of the orbiter depends on the laser transmit power and telescope aperture size. Assuming 0.5 W of power based on LLCD and a 22 cm aperture based on DSOC, the resulting EIRP is 105.42 dBW.

The minimum symbol duration is assumed to be 0.1 ns, which corresponds to the minimum slot size specified in the upcoming CCSDS On-Off Keying standard.

Using these values and Equation 10, we estimate, for instance, that the average number of received photons per second at a reference distance of 100,000 km is $n_s = 1.14$, which results in 2.13 bits per channel use. While these values are a single design point, they can be easily scaled to accommodate different configurations of the optical terminals, as well as changes to the flyby profile.

Figure 2 plots the link analysis results for two exemplary flyby profiles at Mars and Jupiter. For the former, we have assumed the same flyby profile as in Reference [2], which requires $v_1 = 4.31$ km/s and has altitude equal to 17,700 km during closest approach (similar to areostationary orbit). For Jupiter, our preliminary search for cycler orbits yielded candidates requiring $v_1 = 7.13$ km/s and much higher altitude at closest approach when to compared to Mars, up to 1.68 million km approximately. These stark differences in flyby profiles have significant impact on the crosslink between the orbiter and the data mule. In particular, the Mars flyby has an optical crosslink with data rates ranging from 10 to 60 Gbps approximately, which requires each optical symbol to carry between 1.1 and 6 bits. In other words, the link is bandwidth constrained for the entire flyby. Alternatively, the crosslink at Jupiter only operates at 340 Mbps approximately, using less than 0.1 bits per symbol. Therefore, in this case the link is power-constrained.

While the reported numbers in this section are only valid under the present set of assumptions and do not take into consideration technological constraints such as finite code rate options, and laser power and timing limitations, they hint at significant differences when deploying a data mule network at Mars vs. Jupiter. For instance, none of the code rates assumed in this analysis are currently supported by CCSDS standards. Therefore, if a data mule network is to be deployed at Mars, investment in bandwidth-efficient coherent optical modulation systems is required. At Jupiter, on the other hand, we can rely on current PPM technology (direct detection), but standards need to be updated so that lower than 1/2 code rates are available.

4. DATA VOLUME ANALYSIS

Once the link budget assumptions have been laid out, it is now possible to estimate differences in data volume returned using normal DSN operations and a network of data mules. This analysis is performed considering two factors: Cycler orbit phasing in the Earth-Mars/Jupiter synodic cycle; and optical technology available.

Cycler Orbit Phasing

We now consider how the time of arrival of the data mule to Mars and Jupiter affects the effectiveness of our proposed concept. To that end, we estimate $\beta(t_1, t_2)$ assuming that the crosslink uses 1 day of the orbiter operations (i.e., $t_2 = t_1 + 1$ day) during which data transfer occurs for 22 out of 24 hours. Furthermore, we assume that the data mule network is set up such that only one flyby occurs per synodic cycle

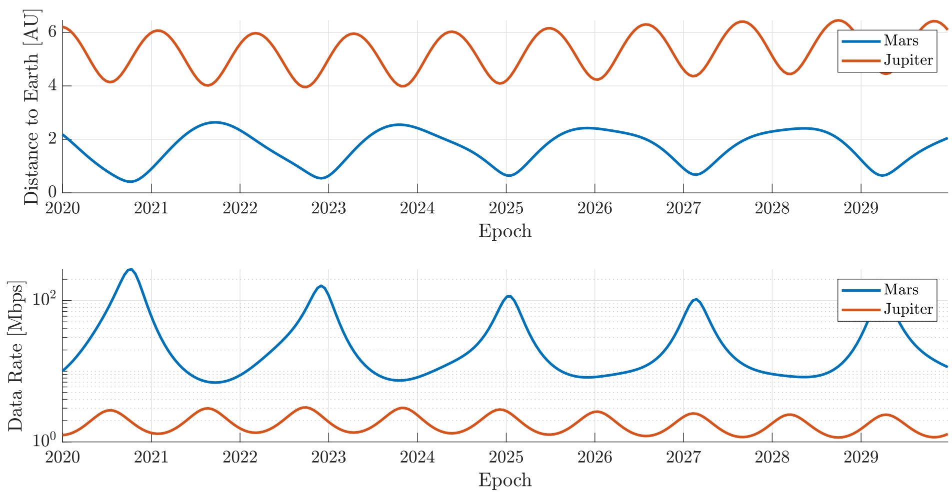

Figure 1: **Data Rate for DTE link**

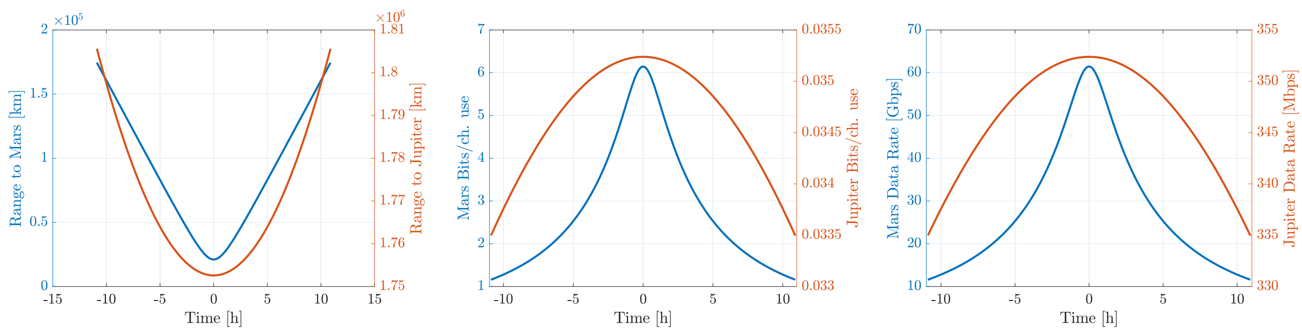

(a) **Flyby Distance** (b) **Crosslink Bits per Channel Use** (c) **Crosslink Data Rate**

Figure 2: **Flyby Link Analysis**

(approximately 2 years for Mars, and 1 year for Jupiter). Note that this is done simply because the relative range between Earth and the planetary body is approximately cyclical with this period. Other constraints such as transit time to the planet might render visits at this cadence impractical in real-life operations.

Figure 3 shows the results of this exercise for Mars and Jupiter. In each case, we plot the distance between Earth and the planet, normalized by its minimum value, as well as β. Results indicate that regardless of the cycler orbit phasing, our proposed system can increase the total data volume by as much as 63% if deployed at Mars, and as much as 43% if deployed at Jupiter. The insensitivity of the results to orbit phasing is due to the fact that forgoing one day of DSN operations to operate the crosslink, even if the flyby occurs on the exact day of minimum Earth-planet range, is not a significant enough disruption to the DTE link that a large data volume is lost. In other words, since the DSN trickles data back to Earth at relatively low speeds compared to the crosslink, the opportunity cost of stopping the DTE link for 24 hours is low.

Finally, note that all results reported so far assume that the link between Earth and the orbiter operates at Ka-band. Since this is currently not the standard for Mars operations, we now consider how β changes when the DTE link runs at X-band. In particular, it can be shown that for an X-band power-constrained link between the orbiter and a DSN 70m antenna,

$$R^{\text{u}}_{\text{rf}} \quad \frac{4.58 \quad 10^6}{d^2} \text{ bps.} \tag{21}$$

Note that this value is one order of magnitude lower than for Ka-band. Therefore, at best we expect β to be 16. In reality, however, we estimate β to be 7.6 for Mars, and 5.6 for Jupiter.

Optical Technology

Next, we focus our attention on the sensitivity of the results with respect to our optical technology assumptions. In particular, three elements are revisited: Laser transmit power, aperture diameter, and symbol duration. Table 1 shows the improvement in β achievable as a function of the available optical crosslink power and bandwidth. Observe that $\beta > 10$ is possible using telescope apertures and powers already in development, provided that the laser bandwidth is increased by one order of magnitude compared to current technology. In other words, our proposed concept is able to return up to 10 times more data volume to Earth than if a deep space downlink at Ka-band was available 24/7 during an entire synodic period. This represents an amortized data volume of 17.2 Tbit/year from Mars, and 0.42 Tbit/year from Jupiter, orders of magnitude more than what is possible today.

Finally, note that the improvement is even more astounding if we compare the data mule network with today's X-band

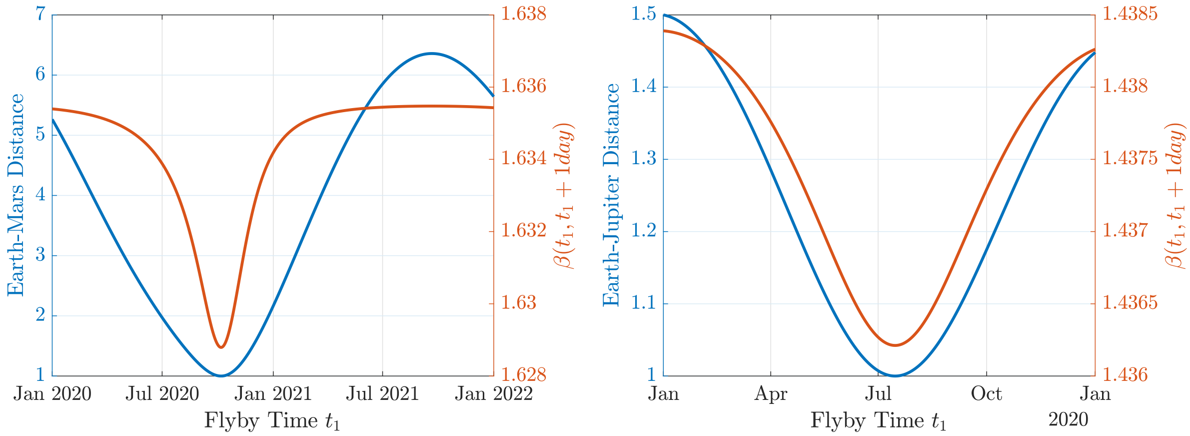

(a) **One Mars flyby every 2 years**

(b) **One Jupiter flyby every year**

Figure 3: **Effect of Orbit Phasing over one Synodic Period**

Table 1: System Performance

Transmitter Power [W]	**Receiver Diameter [m]**	**Symbol Duration [ns]**	**bit/ch use Mars**	β **Mars**	**bit/ch use Jupiter**	β **Jupiter**
0.5	0.1	0.1	2.13	1.6 (x1.00)	0.034	1.4 (x1.00)
0.5	0.22	0.1	4.03	2.1 (x1.31)	0.127	2.6 (x1.86)
4	0.22	0.1	6.92	2.7 (x1.69)	0.609	8.8 (x6.59)
0.5	0.1	0.01	0.53	3.2 (x2.00)	0.005	1.6 (x1.14)
0.5	0.22	0.01	1.45	5.7 (x3.56)	0.018	3.4 (x2.40)
4	0.22	0.01	3.73	11.0 (x6.88)	0.106	14.5 (x10.36)

downlink. In this case, we estimate that the data mule network would be able to return 100 and 140 more data to Earth from Mars and Jupiter, respectively. This is a clear leap in capability that renders our system a good complement to the DSN, even considering its evolution over the next decades.

Additional Considerations

In this last section we briefly comment on two topics that are relevant to our data mule concept but that were not studied in this paper: On-board storage and data latency. For the system to work, both the observer and the courier need to be able to hold large amounts of data in memory for extended periods of time. This is especially challenging in space, where the Earth's magnetosphere does not protect electronics from deep space and solar radiation. Indeed, Jupiter is well known for having a particularly harsh radiation environment. While a detailed analysis of on-board memory is not the focus of our paper, an initial feasibility analysis showed that radiation effects can be mitigated using increased redundancy. Indeed, assuming a memory density similar to that of 2019 commercial cutting edge technology (memory devices used in space typically lag commercial by about 10 years), a memory density of 6.5x10-16 gram/bit, and a total on-board storage of 1 Pb, the total mass required for storage is just 0.7kg. Even with a reliability factor of 40%, this still only comes out to 1kg per Pb.

Another important issue is the latency with which data is delivered to Earth by the data mule system. Due to the need to physically shuttle the data, this latency is expected to be on the order of the duration of a transfer orbit, but exact figures require complicated analyses that depend on the number of cyclers, the spacing of their visits, their launch profile, and many other factors that are fruitful for future research. In [2] this throughput/latency tradeoff was explored more thoroughly for the Mars system and shown that a yearly visit from Mars to Earth could be accommodated with a small number of cyclers, yielding a maximum latency of 12 months. At Jupiter, data latency is expected to be even longer due to larger transit times to and from the planet. While this might seem excessive when compared with the usual latency of hours to days with normal DSN operations, the large volume of "bonus" data provided by the proposed system suggests that cyclers should shuttle lower-priority, larger-area and/or high-resolution datasets (e.g., mineralogical maps or long-horizon time-series) for which latency is not an issue.

5. SUMMARY

This paper studies the concept of data mules in the solar system using two case studies, Mars and Jupiter. Starting from fundamental link capacity equations, we show that our proposed system can increase total data volume returned to Earth by two orders of magnitude compared to current operations. We also show that while this improvement occurs irrespective of which planet we are considering, the technology required to implement the optical crosslink between the orbiter and the data mule is significantly different for Mars and Jupiter. This is due to important differences in the flyby trajectories from the cycler orbits, which result in one link being bandwidth-constrained (Mars) and the other being power-constrained (Jupiter).

The main focus of this paper has been to study the communication performance of the optical crosslink between the orbiter and the data mule, and compare the total returned data volume against what is achievable with the DSN. Several additional dimensions of the trade-space should also be analyzed: First, we did not consider the link between the data mule and Earth, and we did not allow for an optical DTE link. Additionally, all optical link capacity calculations assumed noise-free communications, partially because optical noise at Mars and Jupiter is not well understood, but also because our aim was to obtain upper bounds on system performance to understand if more in-depth analyses are granted. Finally, several considerations related to spacecraft design and trajectory were completely ignored in this paper but are paramount to implement the proposed concept. This includes, for instance, cycler selection and phasing, launch and injection into cycler orbits and memory management on board the data mule.

ACKNOWLEDGMENTS

The research was carried out at the Jet Propulsion Laboratory, California Institute of Technology, under a contract with the National Aeronautics and Space Administration (80NM0018D0004).

APPENDICES

A. OPTICAL CAPACITY APPROXIMATIONS

In this section we provide approximations of the ultimate optical capacity under the assumption of small and large average number of photons per symbol. In particular, if $n_s \ll 1$, then

$$\begin{aligned} (1+n_s)\log_2(1+n_s) &\approx n_s/\ln 2 \\ n_s \log_2 n_s &\approx 0 \end{aligned} \tag{22}$$

where we have used the Taylor expansion $\log(1+x) \approx x$ for small x, and the fact that $\lim_{x \to 0} x \log x = 0$. Therefore,

$$C_{\text{opt}}^{\text{ult}} \approx \frac{n_s}{\ln 2} \left[\frac{\text{bits}}{\text{ch. use}}\right]. \tag{23}$$

Alternatively, when $n_s \gg 1$, we first reorder the terms in the capacity equation as follows

$$\frac{(1+n_s)^{1+n_s}}{n_s^{n_s}} = n_s \left(1 + \frac{1}{n_s}\right)^{1+n_s} \tag{24}$$

and then we let n_s tend to infinity. In that case, $\left(1+\frac{1}{n_s}\right)^{1+n_s}$ tends to e and therefore

$$C_{\text{opt}}^{\text{ult}} \approx \log_2(n_s \cdot e) = \frac{1+\ln n_s}{\ln 2} \left[\frac{\text{bits}}{\text{ch. use}}\right]. \tag{25}$$

B. DATA MULES OPTIMALITY CONDITIONS

In this appendix we derive the optimality conditions that maximize the data mules concept figure of merit. In other words, we solve the following optimization problem

$$\max_{t_1, t_2} \beta(t_1, t_2) \tag{26}$$

where $\beta(t_1, t_2)$ is defined as in Equation (15). To simplify notation, let $\beta(t_1, t_2) = \frac{N(t_1, t_2)}{D(t_1, t_2)}$ and assume that $D(t_1, t_2) > 0$ for all t_1, t_2, as is the case in our problem of interest. In that case, the optimality conditions for t_1 and t_2 can simply written as

$$\begin{aligned} \frac{\partial \beta(t_1, t_2)}{\partial t_1} &= 0 \\ \frac{\partial \beta(t_1, t_2)}{\partial t_2} &= 0, \end{aligned} \tag{27}$$

which yield

$$\begin{aligned} \frac{\partial N(t_1, t_2)}{\partial t_1} D(t_1, t_2) &= N(t_1, t_2) \frac{\partial D(t_1, t_2)}{\partial t_1} \\ \frac{\partial N(t_1, t_2)}{\partial t_2} D(t_1, t_2) &= N(t_1, t_2) \frac{\partial D(t_1, t_2)}{\partial t_2}. \end{aligned} \tag{28}$$

Using Leibniz's rule of differentiation and the numerator and denominator of Equation (15), we get

$$\begin{aligned} \frac{\partial N(t_1, t_2)}{\partial t_1} &= C_{\text{rf}}(t_1) - C_{\text{opt}}(t_1) \\ \frac{\partial N(t_1, t_2)}{\partial t_2} &= 0 \\ \frac{\partial D(t_1, t_2)}{\partial t_1} &= 0 \\ \frac{\partial D(t_1, t_2)}{\partial t_2} &= C_{\text{rf}}(t_1) - C_{\text{opt}}(t_1). \end{aligned} \tag{29}$$

Substituting Equation (29) into Equation (28), yields the following result:

- The optimal value for t_1 can be obtained by solving $C_{\text{rf}}(t_1) = C_{\text{opt}}(t_1)$.
- The optimal value for t_2 can be obtained by solving $C_{\text{rf}}(t_2) = C_{\text{opt}}(t_2)$.

REFERENCES

[1] B. Moision and W. Farr, "Range dependence of the optical communications channel," *The Interplanetary Network Progress Report*, vol. 42, p. 199, 2014.

[2] M. S. Net, E. Pellegrini, and J. Vander Hook, "Cycler orbits and the solar system pony express," in *2020 IEEE Aerospace Conference*. IEEE, 2020, pp. 1–10.

[3] J. H. Yuen, *Deep Space Telecommunications Systems Engineering*. Jet Propulsion Laboratory, 1983.

[4] B. Erkmen, B. Moision, and K. Birnbaum, "The classical capacity of single-mode free-space optical communication: A review," *The Interplanetary Network Progress Report*, vol. 42, p. 179, 2009.